FT-Raman spectroscopic study, aided by quantum chemical DFT calculations, of a series of oligothiophenes end-capped by nitriles

ARTICLE *in* JOURNAL OF MOLECULAR STRUCTURE · JUNE 2005

Impact Factor: 1.6 · DOI: 10.1016/j.molstruc.2004.10.055

8 AUTHORS, INCLUDING:

Maria Carmen Ruiz Delgado
University of Malaga
82 PUBLICATIONS **1,345** CITATIONS
SEE PROFILE

Juan Casado
University of Malaga
227 PUBLICATIONS **3,684** CITATIONS
SEE PROFILE

Victor Hernandez
University of Malaga
172 PUBLICATIONS **2,987** CITATIONS
SEE PROFILE

Juan Teodomiro López Navarrete
University of Malaga
335 PUBLICATIONS **5,234** CITATIONS
SEE PROFILE

Available online at www.sciencedirect.com
SCIENCE DIRECT
Journal of Molecular Structure 744–747 (2005) 403–409
Journal of MOLECULAR STRUCTURE
www.elsevier.com/locate/molstruc

FT-Raman spectroscopic study, aided by quantum chemical DFT calculations, of a series of oligothiophenes end-capped by nitriles

V. Cuberos Guzmán[a], R. Ponce Ortiz[a], M.C. Ruiz Delgado[a], R. Azumi[b], R.T. Oakley[c], J. Casado[a], V. Hernández[a], J.T. López Navarrete[a,*]

[a]*Departamento de Química Física, Facultad de Ciencias, Universidad de Málaga, Málaga 29071, Spain*
[b]*Nanotechnology Research Institute, National Institute of Advanced Industrial Science and Technology, Tsukuba Central 5-2, Higashi 1-1-1, Tsukuba, Ibaraki 305-8565, Japan*
[c]*Department of Chemistry, University of Waterloo, Waterloo, Ont., Canada N2L 3G1*

Received 6 September 2004; accepted 11 October 2004
Available online 7 December 2004

Abstract

We report on the FT-Raman spectroscopic characterization, aided by DFT model chemistry calculations, of a bunch of α,ω-dicyano end-capped oligothiophenes, ranging in length from the dimer to the hexamer, which have been previously shown to display quite promissing amphoteric redox properties for their potential use in new technological applications. The attention is mainly focused to the role played by the CN···H hydrogen bonding interactions between adjacent molecules on various molecular properties, such as the minimum-energy geometry, atomic charges equilibrium distribution,topologies/energies of the frontier molecular orbitals and the Raman scattering spectral profile. To this end we have performed to two sets of quantum chemical calculations, at the DFT//B3LYP/3-21G* level, on: (a) a single terthiophene in the vacuum and (b) a suited dimeric model with a fully coplanar array of the two terthienyl segments interacting through the cyano end-caps.

Keywords: Oligothiophenes; π-Conjugated materials; FT-Raman spectroscopy; DFT calculations

1. Introduction

We investigate herein by means of FT-Raman spectroscopy and DFT model chemistry some α,ω-dicyano end-capped oligothiophenes, which have been previously found to display a interesting amphoteric redox behavior for new technological applications [1]. Oligothiophenes have received great attention over the last decade for their potential use in a variety of molecular electronic and photonic devices, including nonlinear optics [2], Schottky diodes [3], organic light-emitting diodes (OLEDs) [4], and thin-film effect transistors (FETs) [5].

The Raman spectral features of these α,ω-dicyano end-capped oligothiophenes are analyzed with the help of DFT//B3LYP/3-21G* calculations, with the purpose of deriving information about the role played by the CN···H intermolecular interactions on different properties, such as optimal geometry, equilibrium charge distribution, topologies/energies of the frontier molecular orbitals around the gap and the Raman scattering vibrational spectrum from the comparison between the DFT//B3LYP/3-21G* quantities computed for a single terthiophene in the vacuum and for a dimeric model with the fully coplanar array of the two terthenyl mioeties most suited to favour the CN···H intermolecular interactions.

2. Experimental and computational details

The FT-Raman spectra were recorded either on pure solids or dilute solutions in sealed capillaries in a back scattering configuration by means of the FRA 106/S modulus of a Bruker Equinox 55 FT-IR interferometer, operating upon a 1064 nm Raman excitation from an infrared diode pumped Nd-YAG laser. Signal detection

* Corresponding author. Tel.: +34 95 213 1865; fax: +34 952 132000.
E-mail address: teodomiro@uma.es (J.T. López Navarrete).

0022-2860/$ - see front matter © 2004 Elsevier B.V. All rights reserved.
doi:10.1016/j.molstruc.2004.10.055

was carried out by using a germanium detector working at liquid nitrogen temperature.

DFT calculations were carried out with the GAUSSIAN 98 program [6] running on a SGI Origin 2000 supercomputer. Molecular geometry optimizations were performed with the B3LYP functional and the 3-21G* standard basis set [7,8]. All geometrical parameters were allowed to vary independently apart from planarity of the rings. On the resulting ground-state molecular geometries, the harmonic vibrational frequencies and intensities were computed analytically with the same functional. We followed the nowadays rather usual adjustment of theoretical force fields in which 3-21G* theoretical frequencies are uniformly scaled down by a factor of 0.98, as recommended by Scott and Radom [9]. This quite simple scaling procedure, however, is often accurate enough to disentangle serious experimental misassignments. All quoted vibrational frequency values reported along the paper are thus the scaled ones. Theoretical spectra were plotted by convoluting the scaled frequencies with Gaussian functions (10 cm^{-1} width at the half-height). The relative heights of the Gaussians were determined from the DFT//B3LYP/3-21G* Raman activities.

3. Results and discussion

3.1. Optical absorption data

The chemical structures and abbreviate notation of the homologous series of α,ω-dicyano end-capped oligothiophenes studied in this article are depicted in Fig. 1. The synthesis of the oligomers has been reported elsewhere [10].

Table 1 lists the maxima (λ_{max}) of the strong absorption band of each α,ω-dicyano end-capped oligothiophene in the visible spectral region, measured both in CH_2Cl_2 and DMSO solutions. The peak position of this visible absorption, which is attributable to the one-electron π–π* transition, largely redshifts with increasing chain length of the oligomer; the optical absorption data also show that these π-conjugated materials are characterized by a smaller HOMO–LUMO separation than their unsubstituted oligothienyl counterparts. In this regard, the attachment of a pair of electron-withdrawing cyano groups to the end α,ω-positions of the terthienyl induces a bathochromic shift of ≈50 nm. A similar, but larger effect has been previously observed upon dinitro substitution of terthiophene, the redshift being mainly caused by the sizeable stabilisation of the LUMO frontier orbital upon end-capsulation of

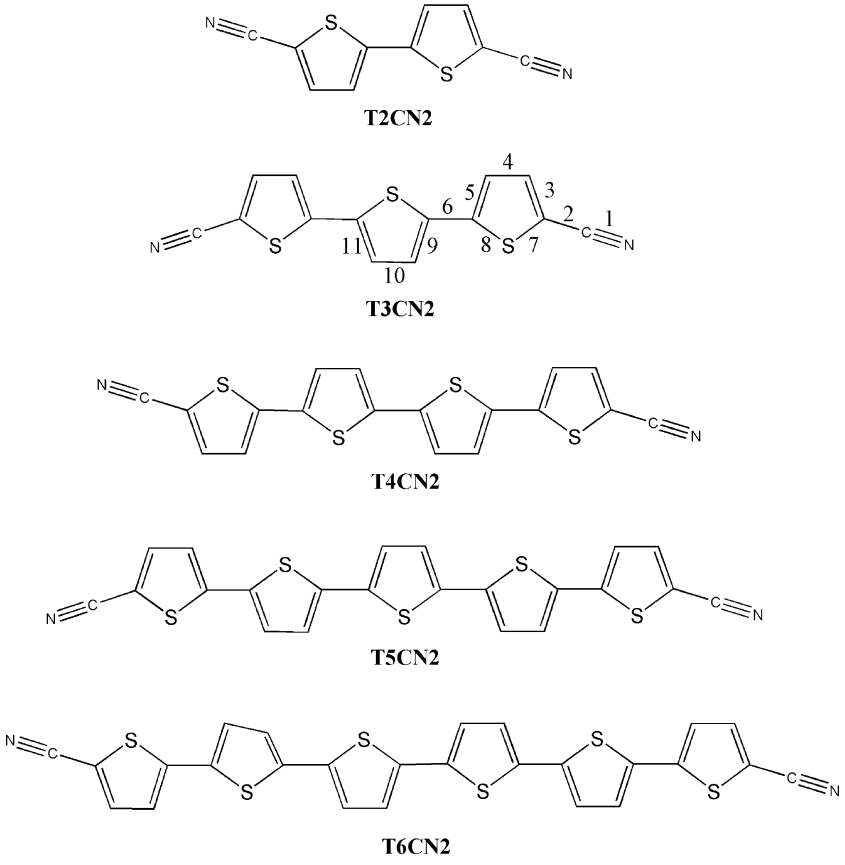

Fig. 1. Chemical structures and abbreviate notation of the various α,ω-dicyano end-capped oligothiophenes under study (the bond numbering of the trimer is to be used in Table 3).

Table 1
UV–Vis absorption maxima (λ_{max}, in nm) associated to the π–π* transition along the series of α,ω-dicyano end-capped oligothiophenes (i.e. measured in CH_2Cl_2 and DMSO solutions)

	CH_2Cl_2	DMSO	Optical band gap
T2CN2	338 (3.67 eV)	344 (3.61 eV)	376 (3.30 eV)
T3CN2	382 (3.25 eV)	390 (3.18 eV)	434 (2.86 eV)
T4CN2	416 (2.98 eV)	424 (2.92 eV)	475 (2.61 eV)
T5CN2	436 (2.84 eV)	444 (2.79 eV)	501 (2.48 eV)

the π-conjugated system with electron-acceptor groups, as deduced from quantum-chemical DFT calculations [11]. Optical band gaps (also listed in Table 1) were approximated by extrapolation of the low energy side of the visible π–π* absorption band to the baseline of each electronic spectrum.

The effect of solvent on the electronic absorption spectra is also outlined in Table 1. The π–π* transition of all the oligomers is found to occur at higher energies in CH_2Cl_2 than in more polar solvents such as DMSO. This spectroscopic behavior is commonly known or termed as positive solvatochromic, and its origin is the greater stabilization of the excited state relative to the ground state with increasing polarity of the solvent [12]. The fact that these α,ω-dicyano end-capped oligothiophenes display solvatochromic properties, although moderate, suggests the occurrence for this class of symmetrically disubstituted systems of a certain degree of intramolecular charge transfer (ICT) from the π-conjugated spine to the cyano end-caps. The topologies of the HOMO and LUMO frontier orbitals should provide a deeper insight into this topic.

3.2. Experimental Raman scattering spectra

The solid-state FT-Raman scattering spectrum of **T3CN2** plotted in Fig. 2, taken as the prototypical example for the other oligothiophenes, evidences the involvement of the cyano end-caps into the π-conjugation (i.e. particularly for the two shorter oligomers, since the ν(CN) Raman line around 2220 cm^{-1} progressively loses in intensity relative to those due to the ν(C=C) stretchings near 1540 and 1450 cm^{-1} on going from **T2CN2** to **T6CN2**). Another key observation is that only three Raman lines at 2219, 1528 and 1456 cm^{-1} are recorded with appreciable intensity for **T3CN2**, in spite that the trimer has 25 atoms and 3N–6 = 69 normal vibrations should be expected to appear in the IR/Raman spectra. The seeming simplicity of the Raman spectral profile of any sort of π-conjugated systems is a well-known phenomenon, that was accounted for more than 15 years ago, among other scientists, by Prof. G. Zerbi and co-workers at the Politecnico di Milano in the framework of the *Effective Conjugation Coordinate (ECC) Theory* by assuming the occurrence in these quasi one-dimensional systems of a very effective electron–phonon coupling, which should lead to the selective enhancement, among the very huge number of Raman-active normal modes predicted by the optical selection rules, of rather a few totally symmetric skeletal ν(CC) stretching and in-plane δ(CH) bending vibrations (i.e. of those molecular vibrations which mostly resemble the structural evolution of the π-conjugated backbone in going from the ground to the first electronic excited state) [13]. This enhancement is clearly observed in the enlarged Raman spectral profile plotted in Fig. 3.

Let us focus our attention to the Raman scatterings appearing in the 2225–2210 cm^{-1} spectral region, due to the ν(CN) stretching normal modes. As can be observed in Fig. 4, which displays the evolution in the solid-state of the peak positions of the ν(CN) Raman lines with the oligomer chain length, there occurs a redshift on going from the dimer to the tetramer and then an upshift to the hexamer: 2222 cm^{-1} (**T2CN2**), 2219 cm^{-1} (**T3CN2**), 2216 cm^{-1} (**T4CN2**), 2216 cm^{-1} (**T5CN2**), and 2221 cm^{-1} (**T6CN2**). It should be in principle expected the ν(CN) Raman lines to appear at

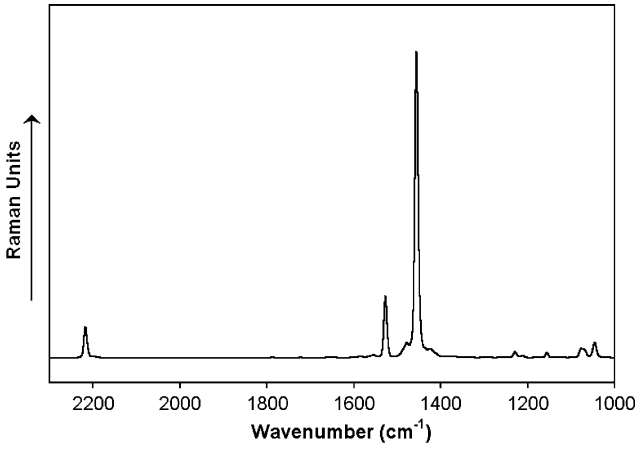

Fig. 2. FT-Raman spectrum of **T3CN2** as a pure solid sample, taken as the prototypical Raman-scattering spectral profile for the whole series of π-conjugated oligomers.

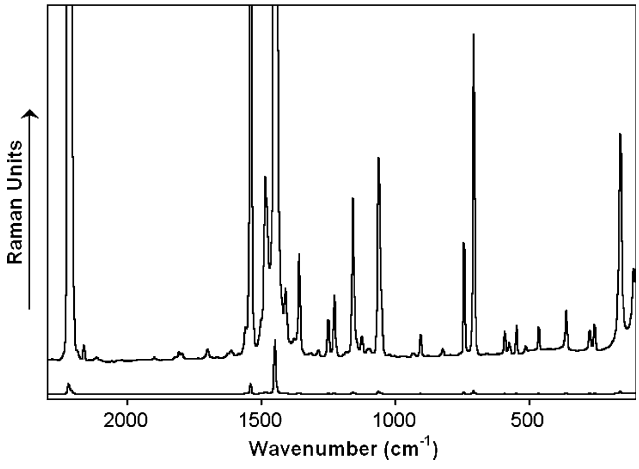

Fig. 3. Enlarged solid-state FT-Raman scattering profile of **T2CN2** in the 2300–100 cm^{-1} spectral region showing the selective enhancement of the lines at 2222, 1542 and 1451 cm^{-1} with respect to the remainder Raman-active vibrations.

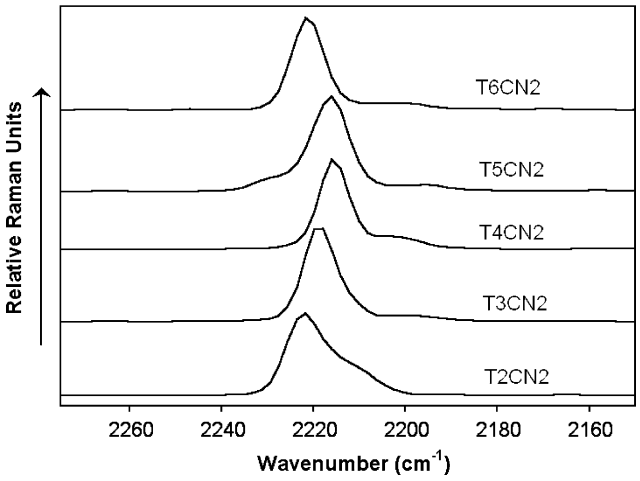

Fig. 4. Chain-length evolution of the peak positions of the solid-state Raman bands due to the ν(CN) stretching vibrations along the whole series of oligothiophenes.

ever lower frequency values as the oligomer grows longer π-electrons, due to the increasing easiness in attracting the π-electrons cloud towards the electron-withdrawing cyano end groups, but this is not the current situation.

The complete single-crystal structural characterisation of this homologous series of oligothiophenes was achieved prior to this work [10]. The analysis of the X-ray diffraction data revealed the main role played by the intermolecular interactions between nitrile groups in generating molecular ribbons in which the adjacent molecules are linked through close CN···H contacts. In addition, these CN···H interactions appeared to be the driving force in determining the ribbon packing. Thus, for the trimer, tetramer and pentamer the ribbon-like arrays adopted slipped π-stack structures rather than the herringbone packing usually found in unsubstituted or α,ω-dialkyl end-capped terthiophene, quaterthiophene, sexithiophene and octathiophene [14]. Only for the hexamer did the packing of the ribbons revert to the herringbone pattern.

We have also observed that for the three shorter oligomers (i.e. the longer ones were found to be little or sparingly soluble) the ν(CN) Raman lines undergo a slight upshift when the pure vacuum-sublimated solids were dissolved in CH_2Cl_2, whereas they slightly downshift upon DMSO solution (experimental frequency values are reported in Table 2, whereas Fig. 5 displays a comparison between the solid-state/solution Raman profiles of **T3CN2** in the 2250–2150 cm^{-1} spectral range). Based only on the spectroscopic intuition, we suspect that the upshift of the ν(CN) Raman lines is due to the disappearance of the CN···H intermolecular interactions upon the removal of the crystal packing forces. On the other hand, the redshift of the ν(CN) scatterings in passing from CH_2Cl_2 to a more polar solvent such as DMSO suggests again, in agreement with the electronic spectra, that the π-conjugated spine partially lends electron-density towards the nitrile end-caps.

Table 2
Frequencies measured for the ν(CN) Raman lines of the three shorter oligomers in passing from the pure solids to the CH_2Cl_2 and DMSO solutions

	Solid state	CH_2Cl_2	DMSO
T2CN2	2222	2223	2220
T3CN2	2219	2220	2217
T4CN2	2216	2219	2217

[a] Values deduced from the electronic spectra in CH_2Cl_2 solution.

3.3. DFT model chemistry calculations

Table 3 summarises the DFT//B3LYP/3-21G* skeletal bond lengths for **T3CN2** and its dimer, hereafter termed as **2T3CN2**. The minimum-energy structure of **2T3CN2** was reached by starting from a two-entities model interacting through two CN···H contacts, in which the geometry of each entity was deduced from that obtained for single **T3CN2** and by fixing an initial 2.6 Å intermolecular distance for each hydrogen-bonding interaction (i.e. as deduced from the experimental X-ray diffraction data). All geometrical parameters of this **2T3CN2** 'dimer' were then allowed to vary independently, with the only constraint of keeping the planarity of each aromatic unit and the dihedral angles determining the all-anti fashion of the two terthienyl segments. The optimal structure for this hypothetic system was that with a fully coplanar arrangement of the two interacting oligothienyl chains and a distance of 2.2 Å between each CN···H contact. From this **2T3CN2** model we learn than the hydrogen-bonding intermolecular interactions give rise only to very subtle changes in the bond lengths closer to the interacting CN groups (i.e. although the greatest variations between **T3CN2** and **2T3CN2** s do not exceed from 0.002 Å), whereas the central and free or 'non-interacting' outermost thiophene rings display almost the same geometry for both **T3CN2** and **2T3CN2**.

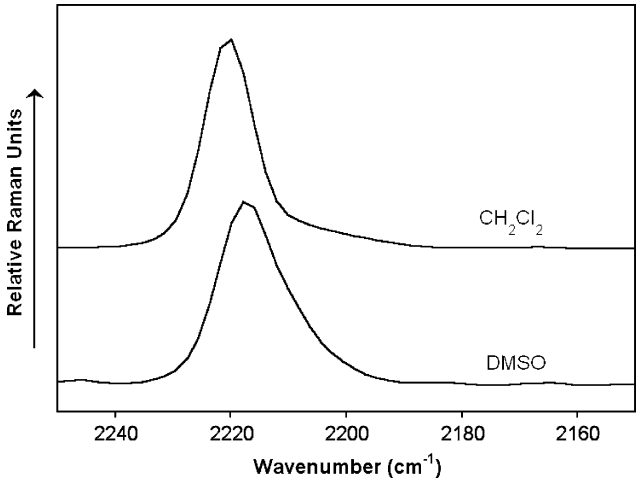

Fig. 5. Detailed peak positions of the ν(CN) Raman scatterings of **T3CN2** in CH_2Cl_2 and DMSO dilute solutions in the 2250–2150 cm^{-1} spectral region.

Table 3
Optimized DFT//B3LYP/3-21G* skeletal bond lengths (in Å) for **T3CN2** and its dimer **2T3CN2** (i.e. bond numbering corresponds to that plotted in Fig. 1)

Bond number	T3CN2	2T3CN2
1	1.168	1.168
2	1.404	1.402
3	1.382	1.383
4	1.415	1.414
5	1.386	1.387
6	1.442	1.442
7	1.750	1.750
8	1.748	1.748
9	1.384	1.384
10	1.415	1.415
11	1.384	1.384
12	1.753	1.752
13	1.753	1.752
14	1.442	1.442
15	1.386	1.386
16	1.415	1.415
17	1.382	1.382
18	1.748	1.748
19	1.168	1.168
20	1.404	1.404
21	1.168	1.168

The distance between the hydrogen and nitrogen atoms of each CN···H pair was fixed to an initial value of around 2.6 Å, as deduced from the X-ray diffraction data, and then was allowed to vary, providing an optimal interacting distance of 2.2 Å.

DFT//B3LYP/3-21G* model chemistry predicts somewhat larger changes regarding the atomic charges equilibrium distributions of **T3CN2** and **2T3CN2**, particularly in the neighbourhood of the interacting cyano groups (see Fig. 6). Main differences between the DFT//B3LYP/3-21G* Mülliken atomic charges computed for the monomer and dimer occur for the C and N atoms of the two interacting nitrile end-caps and the H atoms linked to the nearest β-position of the adjacent coplanar terthienyl moiety, being the S, C_α and C_β atoms around the innermost CN groups of **2T3CN2** those mostly affected by the hydrogen-bonding intermolecular interactions, among all atoms constituting the π-conjugated path. This electrostatic picture reveals the highly local character of the CN···H forces contrarily to the supposedly cooperative character of the intermolecular π–π interactions, which its expect to affect significantly the topologies/energies of the frontier molecular orbitals, and ultimately the electronic/optical properties of the materials from solids to solutions.

Fig. 7 displays the topologies and energies of the frontier molecular orbitals of **T3CN2** and **2T3CN2**. The message coming from these calculations is that the interaction through CN···H contacts (i.e. of electrostatic nature) between two terthienyl moieties arranged in a fully coplanar fashion, does not affect so much the orbitals around the gap in spite that the electron-withdrawing CN groups contribute somewhat to these π-orbitals. In this regard, we see that both the HOMO and LUMO of **2T3CN2** are slightly unstabilized by near 0.06 eV with respect to the single trimer, but both systems should be expected to display similar optical properties. In a future paper we will also address the role played by the face-to-face interactions between parallel oligothienyl moieties (i.e. the π-stacking) in determining the changes of the molecular properties from single entities to cofacial dimers. It seemingly follows that, at least of the shorter oligomers, CN···H interactions are strong enough to drive their solid-state arrangement into the aforementioned ribbon-like structure evidenced in the single crystals, while having only a slight influence on the technologically relevant optical properties of the materials.

DFT//B3LYP/3-21G* model vibrational calculations predict a 2–3 cm^{-1} upshift for the strongest ν(CN) Raman-active normal mode from **T3CN2** to **2T3CN2**

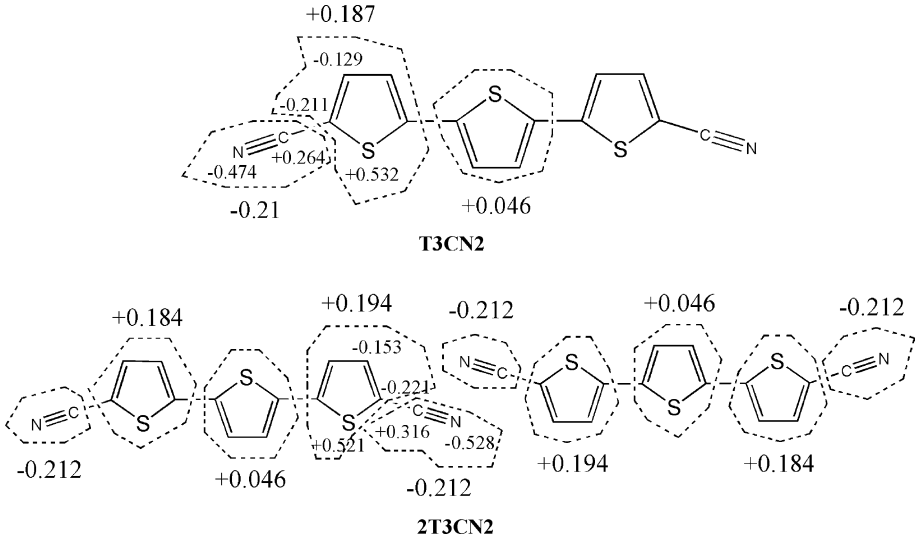

Fig. 6. Overall DFT//B3LYP/3-21G* Mülliken atomic charges over different molecular domains of **T3CN2** and **2T3CN2** and specific values of selected atoms (values are given in *e*).

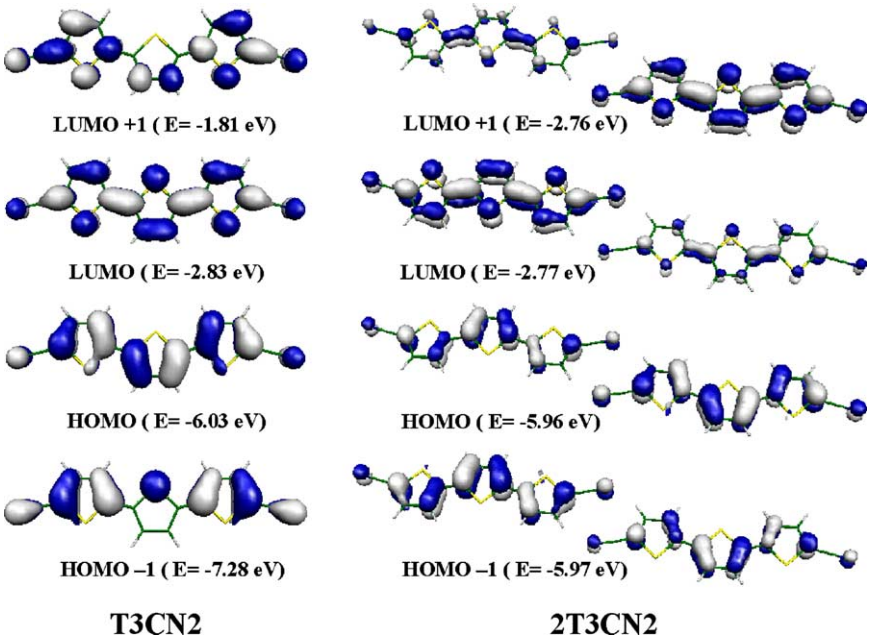

Fig. 7. DFT//B3LYP/3-21G* electronic density contours (0.03 *e*/bohr^3) and energies of the frontier molecular orbitals around the gap for **T3CN2** and **2T3CN2**.

(see Fig. 8). In the dimer, the hydrogen bond interaction with the CN group of the adjacent molecule hinders the CN stretching, thus requiring more energy for the motion, what qualitatively explains the theoretical prediction upon dimerization of the molecule. The totally-symmetric eigenvectors depicted in Fig. 8 reveal that the strongest ν(CN) Raman line in the **2T3CN2** model dimer is strongly located on the two interacting cyano groups, thus pointing to the favoured hydrogen bonding interactions in the shorter oligomers (i.e. those with a ribbon-like structure in the crystal) as the origin of the 'round-trip' observed for the ν(CN) Raman lines with increasing chain length of the α,ω-dicyano end-capped oligothiophene.

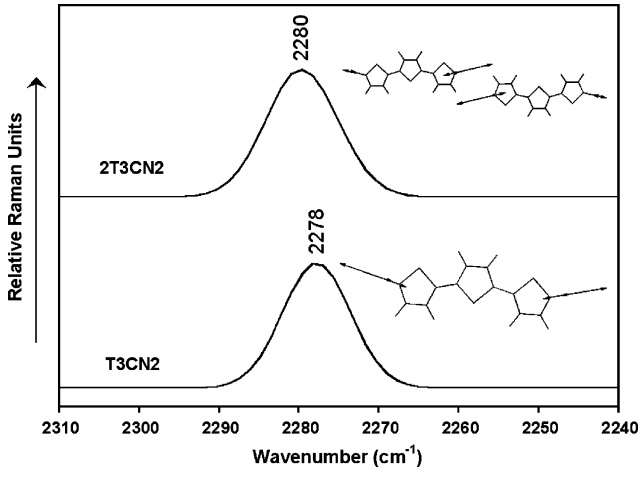

Fig. 8. DFT//B3LYP/3-21G* Raman profiles, in the ν(CN) stretching spectral range, for **T3CN2** and **2T3CN2**, together with the eigenvectors which give rise in each case to the strongest ν(CN) Raman scattering.

4. Summary and conclusions

In summary, we have performed a joint Raman spectroscopy and quantum chemical DFT study of a homologous series of oligothiophenes end-capped by electron-withdrawing cyano groups, paying attention to the analysis of the role played by the intermolecular CN···H interactions. The FT-Raman spectra collected for the pure solid samples evidenced a 6 cm^{-1} redshift for the selectively enhanced ν(CN) scatterings in passing from the dimer to the tetramer, being this frequency downshift fully accounted for in terms of the increasing π-electron density transferred from the ever growing central oligothienyl spine towards the electron-acceptor nitrile end groups. Surprisingly, however, in going from the tetramer to the hexamer the ν(CN) scatterings for the vacuum-sublimated crystalline solids were found to upshift again in spite of the increasing polarizability of the π-electron cloud, so that the experimental peak positions associated to the ν(CN) Raman-active stretchings describes a 'round trip' as the oligomer grows longer.

After the removal of the crystal packing forces, the ν(CN) Raman lines appeared to occur at higher frequency values than in the corresponding solids upon CH_2Cl_2 solution and at lower frequencies when a high polar solvent like DMSO was used. The analysis of the X-ray diffraction data previously published for this bunch of molecular materials resulted to be in full agreement with the two sets of DFT model chemistry calculations reported herein for both: (i) single molecules in the vacuum as well as (ii) suited dimers interacting through short CN···H contacts. The quantum-chemical study of the hydrogen-bonding

interactions revealed that they are strong enough as to drive the solid-state arrangement of the shorter oligomers of the series into an unusual ribbon-like parallel structure, instead of the much more frequently found in crystalline oligothiophenes herringbone structure when π-stacking acts as the main solid-state structural factor. Most of the main molecular properties such as the optimal geometry, atomic charges equilibrium distribution, topologies and energies of the frontier molecular orbitals around the gap and others are, however, slightly or negligibly affected by the CN···H interactions, that thus become quite uselful for tailoring the engineering of the materials at the molecular scale while the potential technological applications based on the relevant electronic and/or optical properties are fully preserved with respect to their unsubstituted oligothienyl counterparts.

Acknowledgements

We acknowledge the Dirección General de Enseñanza Superior (DGES, MEC, Spain) for financial support to this investigation through project BQU2003-03194. The research was also supported by the Junta de Andalucía (Spain) under grant FQM-0159. JC, MCRD and RPO thank the Ministerio de Ciencia y Tecnología (MCyT) and MEC of Spain for a 'Ramón y Cajal' position of chemistry at the University of Málaga (JC) and personal grants (MCRD and RPO).

References

[1] T.M. Barclay, A.W. Cordes, C.D. MacKinnon, R.T. Oakley, R.W. Reed, Chem. Mater. 9 (1997) 981.
[2] F. Geiger, M. Stoldt, H. Schweizer, P. Bäuerle, E. Umbach, Adv. Mater. 5 (1993) 922.
[3] K. Uchiyama, H. Akimichi, S. Hotta, H. Noge, H. Sakaki, Synth. Met. 63 (1994) 57.
[4] G. Horowitz, P. Delannoy, H. Bouchriha, F. Deloffre, J.-L. Fave, F. Garnier, R. Hajlaoui, M. Heyman, F. Kouki, P. Valat, V. Wintgens, A. Yassar, Adv. Mater. 6 (1994) 752.
[5] A.J. Pal, J. Paloheimo, H. Stubb, Appl. Phys. Lett. 67 (1995) 3909.
[6] M.J. Frisch, G.W. Trucks, H.B. Schlegel, G.E. Scuseria, M.A. Robb, J.R. Cheeseman, V.G. Zakrzewski, J.A. Montgomery, R.E. Stratmann, J.C. Burant, S. Dapprich, J.M. Millam, A.D. Daniels, K.N. Kudin, M.C. Strain, O. Farkas, J. Tomasi, V. Barone, M. Cossi, R. Cammi, B. Mennucci, C. Pomelli, C. Adamo, S. Clifford, J. Ochterski, G.A. Petersson, P.Y. Ayala, Q. Cui, K. Morokuma, D.K. Malick, A.D. Rabuck, K. Raghavachari, J.B. Foresman, J. Cioslowski, J.V. Ortiz, A.G. Baboul, B.B. Stefanov, G. Liu, A. Liashenko, P. Piskorz, I. Komaromi, R. Gomperts, R.L. Martin, D.J. Fox, T. Keith, M.A. Al-Laham, C.Y. Peng, A. Nanayakkara, C. Gonzalez, M. Challacombe, P.M.W. Gill, B. Johnson, W. Chen, M.W. Wong, J.L. Andres, M. Head-Gordon, E.S. Replogle, J.A. Pople, GAUSSIAN 98, Revision A.7, Gaussian Inc., Pittsburgh PA, 1998.
[7] A.D. Becke, J. Chem. Phys. 98 (1993) 1372.
[8] W.J. Pietro, M.M. Francl, W.J. Hehre, D.J. Defrees, J.A. Pople, J.S. Binkley, J. Am. Chem. Soc. 104 (1982) 5039.
[9] (a) A.P. Scott, L. Radom, J. Phys. Chem. 100 (1996) 16502;
(b) G. Rauhut, P. Pulay, J. Phys. Chem. 99 (1995) 3093.
[10] T.M. Barclay, A.W. Cordes, C.D. MacKinnon, R.T. Oakley, R.W. Reed, Chem. Mater. 9 (1997) 981 (and references therein).
[11] J. Casado, T.M. Pappenfus, L.L. Miller, K.R. Mann, E. Orti, P.M. Viruela, R. Pou-Amerigo, V. Hernandez, J.T. Lopez Navarrete, J. Am. Chem. Soc. 125 (2003) 2524.
[12] (a) F. Effenberger, F. Wurthner, F. Steybe, J. Org. Chem. 60 (1995) 2082;
(b) C. Reichardt, Chem. Rev. 94 (1994) 2319;
(c) O.-K. Kim, A. Fort, M. Barzoukas, M. Blanchard-Desce, J.-M. Lehn, J. Mat. Chem. 9 (1999) 2227.
[13] (a) C. Castiglioni, J.T. López Navarrete, M. Gussoni, G. Zerbi, Solid State Commun., 65 (1988) 625;
(b) G. Zerbi, C. Castiglioni, M. Del Zoppo, Electronic Materials: The Oligomeric Approach, Wiley-VCH, Weinheim, 1998.p. 345;
(c) V. Hernández, C. Castiglioni, M. Del Zoppo, G. Zerbi, Phys. Rev. B, 50 (1994) 9815;
(d) E. Agosti, M. Rivola, V. Hernández, M. Del Zoppo, G. Zerbi, Synth. Met., 100 (1999) 101.
[14] D. Fichou, J. Mat. Chem. 571 (2000) (and references therein).